Application of stochastic resonance in gravitational-wave interferometer

G. G. Karapetyan
Cosmic Ray Division, Yerevan Physics Institute, Armenia, 375036
(Received 26 October 2005; published 14 June 2006)

We investigate a novel approach which improves the sensitivity of a gravitational-wave interferometer due to the phenomenon of stochastic resonance (SR), performing in a nonlinear cavity (NC). The NC is installed at the output of the interferometer before the photodetector so that the optical signal emerging from the interferometer passes through the NC. Under appropriate circumstances, a specific transformation of the noisy signal inside the NC takes place, which results in the increase of the output signal-to-noise ratio (SNR). As a result, the noisy optical signal of the interferometer becomes less noisy after passing through the NC. The improvement of SNR is especially effective in the bistable NC for wideband (several hundred Hz) detection, when the chirp gravitational-wave signal is detected. Then, for an input SNR of ~ 0.05, the output SNR can be increased up to ~ 0.5. When the detection bandwidth is narrowed, the SR mechanism gradually fades out, and the SNR gain tends to 1. The SNR gain also tends to 1 when the NC is transformed to a linear cavity. Proposed enhancement of the SNR due to SR is not dependent on noise type, which dominates in the interferometer. Particularly, the proposed approach is capable of increasing the SNR at a given amplitude of displacement noise.

DOI: 10.1103/PhysRevD.73.122003 PACS numbers: 04.80.Nn, 02.50.Ey, 05.40.Ca, 95.85.Sz

I. INTRODUCTION

A number of ground-based laser Michelson interferometers are now searching for gravitational waves from different astrophysical objects [1]. Detection of a gravitational wave (GW) is expected to be one of the most exciting scientific results in the near future. It will have important applications both for astronomy, where new information about astrophysical objects will be obtained, and for fundamental physics, where some aspects of general relativity theory can be tested. Among the most likely detectable sources of the GWs are binary systems containing neutron stars and/or black holes [2]. Regardless of the specific configuration, all GW interferometers use the principle of Michelson interferometer to detect the changes $\Delta L = L_1 - L_2$ of the length L in the two perpendicular arm lengths L_1 and L_2. The first generation of GW interferometers having strain sensitivity $\Delta L/L \sim 10^{-21}$ is predicted to detect only large gravitational events. The second generation of detectors, such as the advanced Laser Interferometer Gravitational-Wave Observatory (LIGO) [3] is expected to reach an order of higher sensitivity in the frequency range of several hundred Hz. These instruments will employ higher power lasers, a signal recycling technique, more advanced core optics, and a suspension system. Along with the investigations of these problems, numerous theoretical studies have been carried out suggesting novel approaches and principles. These include the squeezed light [4], the quantum demolition technique [5], the optomechanical coupling technique [6], the Sagnac interferometer [7], white-light cavities [8], stochastic resonance (SR) [9], and more.

The concept of stochastic resonance was originally introduced in 1981 [10], and since then it has continuously attracted growing attention. SR has been studied in biological systems, information theory, chemical reactions, etc., and due to its simplicity and robustness it has established itself as a large area in noise research. Stochastic resonance is a specific transformation of a noisy signal in a nonlinear system, with subthreshold inputs, when output signal content is improved by the assistance of noise. As it is known, output signal-to-noise ratio (SNR) of a linear system decreases when the input noise increases. However, in a nonlinear bistable system the opposite relationship can be observed, i.e., the addition of some noise in the input can *enhance* output SNR, rather than reduce it. Such enhancement takes place in some interval of input noise amplitudes. For low noise amplitudes, the signal does not cause the device to cross the threshold, because so little signal is passed through it as it passes through the linear system. For large noise amplitudes the influence of bistability is not essential, and again the output SNR is close to the input one. However, for moderate amplitudes, the noise allows the signal to cross the threshold coherently to signal time variations, and as a result the output signal becomes more coherent to the input signal, and the output SNR increases. Thus, the response of the system where the SR mechanism is performed will exhibit resonancelike behavior versus the amplitude of input signal's noise, hence the name ''stochastic resonance.''

In the present paper we study the application of SR in a GW interferometer for improving sensitivity. To employ the SR phenomenon, one needs to have a nonlinear system where the noisy signal would be transformed and improved. Earlier in [9] we considered this problem; however, the proposed configuration of the interferometer was not suitable for experiments. In [9] we suggested that the optical nonlinear medium be inserted in the interferometer

arm cavities to turn them into nonlinear cavities and to trigger SR. But such a scheme has the following drawbacks: (i) because of the high power circulating in the arm cavities, it would be difficult to maintain the nonlinear medium in a stable state, and (ii) it would be difficult to provide identical nonlinear parameters for two arm cavities. The scheme suffered also from the necessity of using a special white-light cavity to relax the tight requirements of laser frequency stability.

Here, we consider another, simpler configuration, where an additional nonlinear cavity (NC) is installed in the interferometer output before the photodetector. A sketch of the proposed configuration is shown in Fig. 1. The function of the NC is to improve the SNR of the noisy signal passing through it by the SR mechanism. This scheme is easy to construct in existing ground based interferometers. We present in this paper the results of a theoretical study of such an interferometer. The main motivation of this work was to attract the attention of GW interferometery experts to the SR phenomenon by showing in a simple scheme the feasibility of a SR application for upgrading GW interferometers.

Section II contains the calculations of NC transmittance and the SNR of the input and output noisy signals. In Sec. III, the SNR gain is studied for the sinusoidal GW signal, and in Sec. IV the SNR gain is studied for the chirp GW signal of the binary system.

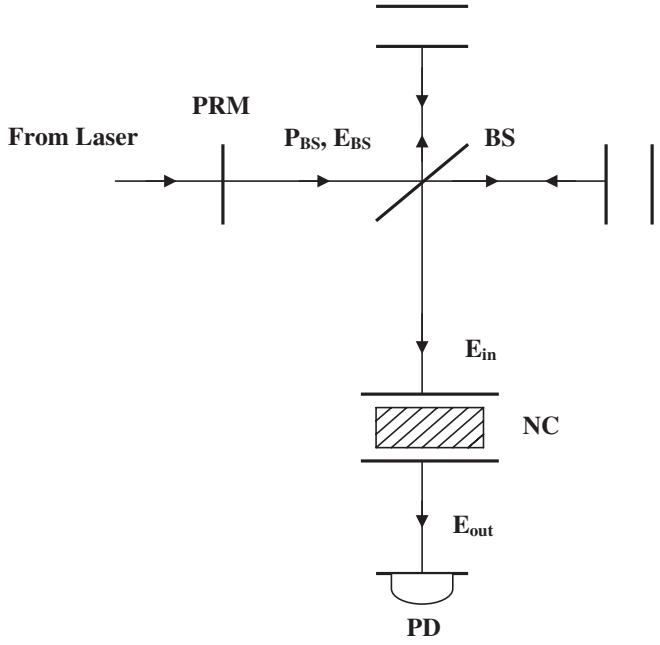

FIG. 1. Schematic of the proposed interferometer's configuration. PRM is the power recycling mirror, BS is the beam splitter, NC is the nonlinear cavity, PD is the photodetector, P_{BS} and E_{BS} are the power and amplitude of electric field incident on the beam splitter, E_{in} is the amplitude of the beam incident on the NC, and E_{out} is the amplitude of the beam emerging on the NC.

II. THE TRANSMITTIVITY OF THE NONLINEAR CAVITY

To investigate the possibility of the NC to improve the SNR of the noisy signal, one needs to derive the relationship between the output (E_{out}) and input (E_{in}) signal amplitudes. We will use the appropriate analytical approach, presented in [9] and based on coupled waves equations [11]. Suppose that the NC is formed by two mirrors placed at $z = 0$ and $z = D$. Each mirror has intensity reflection and absorption coefficients r^2 and w^2 respectively, so that intensity transmittivity of each mirror is $t^2 = 1 - r^2 - w^2$. Region $z_1 < z < z_2$ inside the NC is filled with a nonlinear medium with refractive index $n = n_0 + n_2|E_m|^2$, where n_0 is the background refractive index, n_2 is the nonlinear coefficient, and E_m is the amplitude of electric field of the waves inside the nonlinear medium. The output beam of the interferometer, having power P_{in} and amplitude of electric field E_{in} is incident on the NC. This beam can be described as a quasimonochromatic plane wave, with the electric field given as $E_{in}\exp[i(kz - 2\pi f_{las}t)]$, where $k = 2\pi f_{las}/c$ is the wave number, f_{las} is the laser frequency, and c is the speed of light in vacuum. The electric field inside the NC is written as

$$\begin{aligned} &C_1\exp(ikz) + C_2\exp(-ikz) \quad \text{in } 0 < z < z_1, \\ &D_1\exp(ikz) + D_2\exp(-ikz) \quad \text{in } z_2 < z < D, \\ &U(z)\exp(iknz) + V(z)\exp(iknz) \quad \text{in } z_1 < z < z_2. \end{aligned} \tag{1}$$

Here C_1, C_2, D_1, and D_2 are constant complex amplitudes, and $U(z)$ and $V(z)$ are slowly varying amplitudes inside the nonlinear medium, which obey the coupled waves equations [11]

$$\begin{aligned} &iU'(z) + kn_2U(z)[|U(z)|^2 + 2|V(z)|^2] = 0, \\ &iV'(z) - kn_2U(z)[|V(z)|^2 + 2|U(z)|^2] = 0. \end{aligned} \tag{2}$$

The solutions of (2) can be presented as

$$\begin{aligned} U(z) &= u\exp[i(\alpha z + \alpha_0)], \\ V(z) &= v\exp[i(\beta z + \beta_0)], \end{aligned} \tag{3}$$

where $\alpha = kn_2(u^2 + 2v^2)$, $\beta = -kn_2(v^2 + 2u^2)$, and u and v are real positive constants.

We have four boundary conditions for the electric and magnetic field at nonlinear medium boundaries, and four equations for reflected and transmitted amplitudes at $z = 0$ and $z = D$. Thus a system of eight complex equations is formed, which determines the amplitude of the electric field inside and outside the NC.

After appropriate transformations analogously to [9], the following equation connecting the output E_{out} and input E_{in} amplitudes is obtained:

$$\theta^2E_{out}^6 + 2\theta\delta t^2E_{out}^4 + (\delta^2 + t^4)t^4E_{out}^2 - 4t^8E_{in}^2 = 0, \tag{4}$$

where $\theta = 6\pi d(1 + r^2)n_2f_{las}/c$, $d = z_2 - z_1$ is the thick-

ness of the nonlinear medium, $\delta = 4\pi D(f_{las} - f_{cav})/c$, and $f_{cav} = 2\pi mc/D$ (m is an integer) is the resonance frequency of the empty cavity, closest to the laser frequency.

Substituting in (4) a new variable Y as

$$E_{out} = \sqrt{Y - \frac{2t^2\delta}{3\theta}}, \tag{5}$$

we come to the cubic equation

$$Y^3 + pY + q = 0, \tag{6}$$

with coefficients

$$p = \frac{t^4(3t^4 - \delta^2)}{3\theta^2}, \qquad q = -\frac{2t^6[\delta(\delta^2 + 9t^2) + 54t^2\theta E_{in}^2]}{27\theta^3}. \tag{7}$$

The solutions of Eq. (6) are given by Cardano's formula

$$Y_1 = a + b, \qquad Y_2 = \frac{a+b}{2} + i\sqrt{3}\frac{a-b}{2}, \qquad Y_3 = \frac{a+b}{2} - i\sqrt{3}\frac{a-b}{2}, \tag{8}$$

where

$$a = \sqrt[3]{-\frac{q}{2} + \sqrt{Q}}, \qquad b = \sqrt[3]{-\frac{q}{2} - \sqrt{Q}}, \qquad Q = \left(\frac{p}{3}\right)^3 + \left(\frac{q}{2}\right)^2. \tag{9}$$

It can be checked that $Q > 0$, so Y_1 is always real, whereas Y_2 and Y_3 are real only if $p < 0$ and $E_1 < E_{in} < E_2$, where

$$E_1 = \frac{\theta}{2t^4}\sqrt{q + \frac{4t^8E_{in}^2}{\theta^2} - \sqrt{-\frac{4p^3}{27}}}, \qquad E_2 = \frac{\theta}{2t^4}\sqrt{q + \frac{4t^8E_{in}^2}{\theta^2} + \sqrt{-\frac{4p^3}{27}}}. \tag{10}$$

E_1 and E_2 are defined as the lower and upper thresholds of bistable cavity, respectively, and $E_0 = (E_1 + E_2)/2$.

If we define $f_0 = f_{cav} - 3^{1/2}t^2c/4\pi D$, then $p >= 0$ is equivalent to $f_{las} >= f_0$. In this case E_{out} is described only by the solution Y_1, being a single-value function of E_{in} [see Figs. 2(a) and 2(b)]. However if $f_{las} < f_0$ and $E_1 < E_{in} < E_2$, the E_{out} becomes bistable, which means that at a given input amplitude E_{in}, the E_{out} can get two different values, either in the upper or the lower branches [see Fig. 2(c)]. In this case E_{out} is described by both solutions Y_1 and Y_2, which form together upper and lower branches. This behavior of E_{out} has been observed in experiments [12]. Notice that the third solution Y_3 describes the middle branch—shown in Fig. 2(c) by the dashed line. This is the unstable solution, so E_{out} is never observed on the middle branch. The value of E_{out} hops from the lower branch to the upper one and vise versa as shown in Fig. 2(c), when E_{in} varies with an amplitude larger than the bistability interval $E_2 - E_1$. If E_{out} initially lies say on the lower branch, it remains there until E_{in} crosses the upper threshold E_2. Then E_{out} hops to the upper branch and remains there until E_{in} crosses the lower threshold E_1. Thus, the typical hysteresis phenomenon in the E_{out} versus E_{in} relationship is established if $f_0 > f_{las}$. In order to act effectively, the SR mechanism should have E_{in} varying within bistability interval $E_1 \ldots E_2$. However, as it is known the GW interferometers work in the dark fringe regime, i.e. $E_{in} = 0$ in the absence of a GW induced signal. Hence we assume here that in the absence of a GW induced signal, E_{in} has a constant mean value E_{mean}. This can be provided by a small shift of the beam splitter position or by extracting some portion of the laser beam and directing it to the NC along with the E_{in}. We assume that $E_{mean} = E_0 = (E_1 + E_2)/2$. Under the action of GW with the strain $h(t)$ the length of one cavity changes on $\Delta L(t) = h(t)L$, while the length of another cavity changes on $-\Delta L(t)$. These changes produce a phase shift $\Delta\Phi(t)$ between the two beams reflected from arm cavities. In the result, E_{in} becomes

$$E_{in} = E_0 + \Delta E_{in}(t), \qquad \Delta E_{in}(t) = \Delta E_{GW}(t) = \frac{E_{BS}}{2}\Delta\Phi(t), \qquad \Delta\Phi(t) = 16F\frac{L}{\lambda}\frac{1}{\sqrt{1 + (4\pi\nu\tau)^2}}\frac{\Delta L(t)}{L}. \tag{11}$$

where E_{BS} is the amplitude of the beam incident on the beam splitter, $F = \pi(r_1r_2)^{1/2}/(1 - r_1r_2)$ is the arm cavity finesse, and r_1, r_2 are amplitude reflection coefficients of

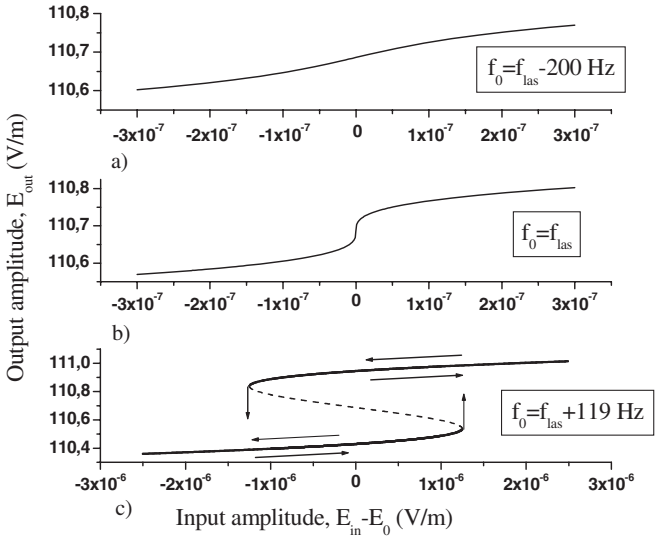

FIG. 2. Output amplitude of the light passing through the NC versus the input amplitude. $D = 10$ cm, $d = 1$ cm, $n_2 = 10^{-13}$ (m/V)^2, $r = 0.99$, and $E_0 = 63.9054261$ V/m.

arm cavity input and rear mirrors. $\lambda = c/f_{las}$ is the wavelength of laser light, ν is GW frequency, $\tau = 2FL/c$ is the arm cavity storage time, and $\Delta L(t)$ is the change of arm cavity length L. Taking into account also the noise of the interferometer, the expression for $\Delta E_{in}(t)$ is written as

$$\Delta E_{in}(t) = \Delta E_{GW}(t) + \xi_{in}(t), \tag{12}$$

where $\xi_{in}(t)$ is the noise signal emerging from the interferometer and incident on the NC. This signal contains all components of the interferometer noise, including displacement noise, shot noise, and photon pressure noise.

To derive the SNR of $E_{in}(t)$, one should calculate separately the spectrum $S_{in}(f)$ of signal + noise and the spectrum $N_{in}(f)$ of noise as the following (the constant E_0 can be omitted in calculations):

$$\begin{aligned} S_{in}(f) &= \int_{t_1}^{t_2} \Delta E_{in}(t) \exp(2\pi i f t) dt, \\ N_{in}(f) &= \int_{t_1}^{t_2} \xi_{in}(t) \exp(2\pi i f t) dt, \end{aligned} \tag{13}$$

where $t_2 - t_1$ is the duration of the GW signal.

Then the input SNR, i.e. the SNR of a signal emerging interferometer and incident on the NC is determined as

$$\mathrm{SNR}_{in} = \left| \frac{\int_{f_1}^{f_2} [S_{in}(f) - N_{in}(f)] df}{\int_{f_1}^{f_2} N_{in}(f) df} \right|^2, \tag{14}$$

where $f_2 - f_1$ is the detection bandwidth.

An analogous equation is written for the output SNR, i.e. the SNR of a signal emerging on the NC:

$$\mathrm{SNR}_{out} = \left| \frac{\int_{f_1}^{f_2} [S_{out}(f) - N_{out}(f)] df}{\int_{f_1}^{f_2} N_{out}(f) df} \right|^2, \tag{15}$$

where

$$\begin{aligned} S_{out}(f) &= \int_{t_1}^{t_2} E_{out}(t) \exp(2\pi i f t) dt, \\ N_{out}(f) &= \int_{t_1}^{t_2} \xi_{out}(t) \exp(2\pi i f t) dt, \end{aligned} \tag{16}$$

and $\xi_{out}(t)$ is the time variation of the noise amplitude at the output of the NC. It is derived from $\xi_{in}(t)$ by the same equations which compute E_{out} versus E_{in}.

SNR gain G of the noisy signal passing through the NC is therefore

$$G = \frac{\mathrm{SNR}_{out}}{\mathrm{SNR}_{in}}. \tag{17}$$

For further numerical analysis one should specify the parameters of the interferometer and the NC. We will use values close to those of LIGO-1 [3]: $L = 4$ km, $P_{las} = 5$ W, $P_{BS} = 150$ W, $F = 100$, and $\tau = 0.9$ ms. The value $E_{BS} = 7.6$ kV/m is found from P_{BS} by using the formula $E_{BS} = (960 P_{BS})^{1/2}/d_B$ for a uniform circular beam with diameter $d_B = 0.05$ m. Then the dependence between $\Delta E_{GW}(t)$ produced in the interferometer output and the change of arm cavity length $\Delta L(t)/L$ under the action of GW with the frequency $\nu = 150$ Hz is given numerically as

$$\Delta E_{GW}(t) = 1.3 \cdot 10^{16} \Delta L(t)/L, \tag{18}$$

where $\Delta E_{GW}(t)$ is measured in V/m.

To drive the SR mechanism, we need to choose the parameters of the NC so that $\Delta E_{GW}(t)$ will vary within the bistability interval $E_2 - E_1$.

A key problem in the building of the NC is the nonlinear medium, which should have a rather high value of the nonlinear coefficient n_2. Recent investigations showed a new possibility of creating such a medium on the basis of the electromagnetic induced transparency phenomenon [13]. The obtained value of n_2 is $\sim 10^{-13}$ $(\mathrm{m/V})^2$. We will use this value of n_2 as well as the following arbitrary parameters: $d = 1$ cm, $r = 0.99$, and $D = 10$ cm. The NC length D is tuned so that $f_0 = f_{las} + 119$ Hz. Then the bistable regime in the NC is established with $E_0 = 63.9054261$ V/m and $E_2 - E_1 = 2.5^* 10^{-6}$ V/m. The appropriate curve of E_{out} versus E_{in} is shown in Fig. 2(c). Note that the relative instability of E_{mean}, which is necessary to have in order to maintain E_{mean} sufficiently close to the E_0 is $\sim (E_2 - E_1)/E_0 \sim 4^* 10^{-8}$. Since E_{mean} is formed by the interference of two arm beams at the beam splitter, the same value of relative instability is transformed to each beam power and to P_{BS} as well. As a result, the required relative instability of laser power, which is necessary to have in order to maintain the position of E_{mean} sufficiently close to the E_0 is $\sim 4^* 10^{-8}$, which is easy to provide.

Now we need to determine the function $\xi_{in}(t)$ as well for computation of $S_{in}(f)$ and $N_{in}(f)$ by Eqs. (13). However. neither analytical expressions nor experimental data describing the time variation of the interferometer noise $\xi_{in}(t)$ is known. Instead, one should derive $\xi_{in}(t)$ from a well-known frequency spectrum of interferometer noise by using an inverse Fourier transform. For this purpose we will use a sample of noise spectrum, which is close to the LIGO-1 noise spectrum [3]. First we approximate the exact numerical data of the noise spectrum by composing the function $F(f)$

$$F(f) = 10^{-23} \left(\frac{400\,000}{f^{2.65}} + 0.015 f \right),$$

where f denotes frequency in Hz.

As shown in Fig. 3(a), the function $F(f)$ well fits exact experimental points of the LIGO-1 noise spectrum up to 1000 Hz. Then, $N_{in}(f)$ is presented as the product of $F(f)$ and a random function $g(f)$

$$N_{in}(f) = F(f) g(f). \tag{19}$$

Here $g(f)$ is a Gaussian random function with mean 0 and mean square value 0.5. The function $N_{in}(f)$ is shown in Fig. 3(b).

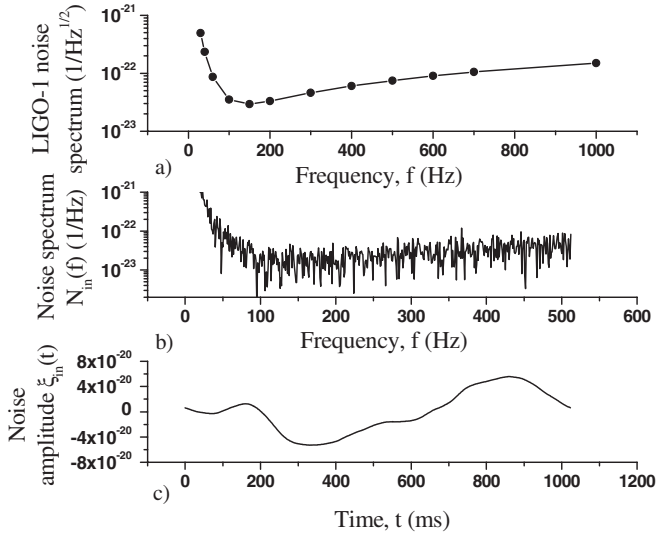

FIG. 3. (a) Discrete values of the noise spectrum, close to those of LIGO-1 (circles) and function $F(f)$, approximating these values (solid line). (b) Composed noise spectrum $N_{\text{in}}(f)$, which is close to the LIGO-1 noise spectrum. (c) Time variation of noise amplitude $\xi_{\text{in}}(t)$, which is close to the time variation of the LIGO-1 noise.

Now supposing that $N_{\text{in}}(f)$ is the noise spectrum of the interferometer, we use an inverse Fourier transform of $N_{\text{in}}(f)$ and obtain the time variation $\xi_{\text{in}}(t)$ of the interferometer noise

$$\xi_{\text{in}}(t) = \frac{1}{2\pi}\int_{-\infty}^{\infty} N_{\text{in}}(f)\exp(-2i\pi ft)df. \qquad (20)$$

Numerical integration of (20) is done in frequency interval $(-512\ldots512)$ Hz by using a fast fourier transform algorithm with 1024 points. As a result we derived the function $\xi_{\text{in}}(t)$, which is close to the time variation of the LIGO-1 noise [see Fig. 3(c)].

Slow drift of the noise amplitude, seen in Fig. 3(c), is conditioned by low frequency components in noise spectrum. This drift will deteriorate the performance of the SR because signal amplitude will frequently move outside of the bistability interval $E_1 \ldots E_2$. To prevent this drift, an appropriate compensation technique should be used. In such compensation, an error signal is generated, which is proportional to the difference between E_{mean} and E_0. This signal is fed back to the actuators to control the amplitude of E_{mean}, locking it to E_0. Another variant of compensation is to control the resonance frequency f_{cav}, controlling by this the bias δ. Then according to (10) E_1 and E_2 will be controlled, and therefore E_0 also will be controlled and locked to the E_{mean}. The faster the response of the compensation loop the higher is the cutoff frequency f_{cut} up to which spectral components of the interferometer noise $\xi_{\text{in}}(t)$ are suppressed. Depending on the quality of the compensation scheme, spectral components below f_{cut} can be either completely removed or suppressed. We will

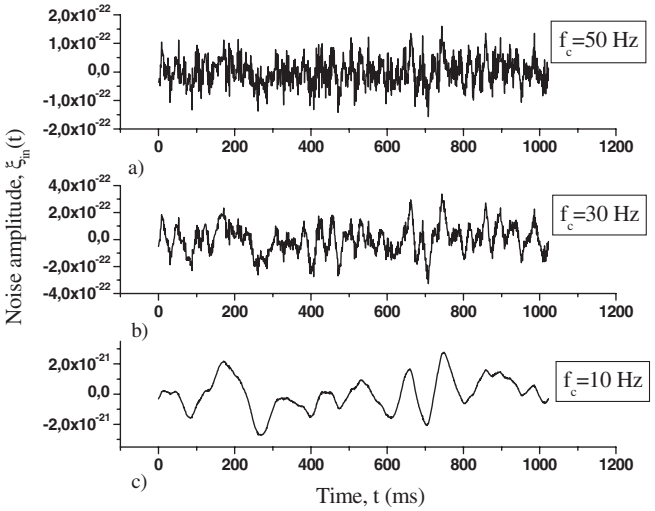

FIG. 4. Time variation of the noise amplitude $\xi_{\text{in}}(t)$ at the different values of cutoff frequencies of the compensation scheme.

assume that the compensation scheme provides the suppression of the noise spectral components below f_{cut} to the value $F(f_{\text{cut}})$. Thus the function $F(f)$ is replaced by another function $F_{\text{comp}}(f)$, when a compensation scheme is implemented, i.e. instead of (19) we have

$$N_{\text{in}}(f) = F_{\text{comp}}(f)g(f)$$
$$F_{\text{comp}}(f) = \begin{cases} F(f) & \text{if } f > f_{\text{cut}} \\ F(f_{\text{cut}}) & \text{if } f < f_{\text{cut}}. \end{cases} \qquad (21)$$

Computing $\xi_{\text{in}}(t)$ according to (20) we obtain the time variation of the noise amplitude $\xi_{\text{in}}(t)$ under the performance of the compensation scheme. As it is seen from Fig. 4 the drift of noise $\xi_{\text{in}}(t)$ for $f_{\text{cut}} = 30$ Hz is about 4^*10^{-22}, which is equivalent to the drift of E_{mean} on about 5.2^*10^{-6} V/m. For $f_{\text{cut}} = 50$ Hz these drifts are correspondingly $\sim 2^*10^{-22}$ and $\sim 2.6^*10^{-6}$ V/m.

III. SINUSOIDAL GW

In this section we investigate the SNR gain when a GW with sinusoidal waveform is detected. Such GWs are emitted by rotating neutron stars or by a binary system, long before the coalescence. The change of arm cavity length is presented as

$$\frac{\Delta L(t)}{L} = A\sin(2\pi\nu t). \qquad (22)$$

Suppose that $A = 10^{-23}$, $\nu = 150$ Hz, and detection bandwidth is $f_2 - f_1 = 450$ Hz $- 50$ Hz $= 400$ Hz. Then the noisy signal

$$\Delta E_{\text{in}}(t) = 1.3\cdot 10^{-7}\sin(2\pi\nu t) + \xi_{\text{in}}(t) \qquad (23)$$

is produced in the output of the interferometer according to (11) and (12). The signal-to-noise ratio of this signal (i.e. SNR_{in}) is calculated by (12)–(14), where $\xi_{in}(t)$ is computed by (20) and (21). The calculations are performed according to the following.

After the generating of 1024 values of the random function $g(t)$, the noise spectrum $N_{in}(f)$ is calculated by using (21) and then by using (20)—the function $\xi_{in}(t)$. Substituting $\xi_{in}(t)$ in (23) we calculate the time variation of the interferometer output signal $\Delta E_{in}(t)$, which is used in (13) to derive the spectrum $S_{in}(f)$ of the interferometer output signal. Finally SNR_{in} is computed from (14). However, the obtained value of SNR_{in} [let it be defined as $SNR_{in}^{(1)}$] can differ from the real experimental value of SNR_{in} because we have used the random function $g(f)$. Therefore, the SNR_{in} calculation procedure should be performed again: the computation code generates a new series of 1024 values of the function $g(f)$ and a new $SNR_{in}^{(2)}$ is derived. Repeating this procedure many times we obtain different values of $SNR_{in}^{(i)}$, $i = 1, 2 \ldots K$. Then the robust value of SNR_{in} is obtained by averaging these values:

$$SNR_{in} = \frac{1}{K} \sum_{i=1}^{K} SNR_{in}^{(i)}. \quad (24)$$

The number of trials K should be chosen such that addition of a new value $SNR_{in}^{(K+1)}$ does not significantly change SNR_{in} in (24). As it is seen from Fig. 5, it is sufficient to take $K \sim 30$. Then the value of SNR_{in} proves to be ~ 0.21. The SNR_{out} is calculated analogously by using the Eqs. (15) and (16). However, it is necessary to use a larger number K, so we took $K = 1000$.

First, let us investigate the dependence of G on the bistability interval $E_2 - E_1$. As it was mentioned earlier, this interval is determined by the bias between the laser frequency f_{las} and f_0 according to (7) and (10). Hence the change of the interval $E_2 - E_1$ can be provided by the change of f_{cav}, which can be done by tuning of the NC length D. In Fig. 6 the SNR gain G versus the length of the bistability interval is plotted. Significant gain of ~ 4 is seen at the value $E_2 - E_1 \sim 2.5^{*}10^{-6}$ V/m. When $E_2 - E_1$ surpasses $2.5^{*}10^{-6}$ V/m, the gain drops sharply to ~ 1. It also decreases to 1 when $E_2 - E_1$ tends to 0 and NC becomes monostable. Such resonance behavior of the SNR gain versus the bistability interval is just caused by the SR mechanism, which performs here according to the following.

When $E_2 - E_1 \gg \Delta E_{in}(t)$ [in our case $\Delta E_{in}(t) \sim 2.5^{*}10^{-6}$ V/m], the $E_{out}(t)$ is localized on one of the branches, so the relationship between E_{out} and E_{in} is approximately linear, and $G \sim 1$. By decreasing $E_2 - E_1$, this linear relationship is preserved until $E_2 - E_1 \sim \Delta E_{in}(t)$. However, as soon as $\Delta E_{in}(t)$ begins to cross the upper E_2 and lower E_1 thresholds and E_{out} begins to hop from one branch to another one, the ratio E_{out}/E_{in} sharply increases. Although crossing of the thresholds and the hops of E_{out} takes place due to the net input noisy signal $\Delta E_{in}(t)$, the content of the GW induced signal in E_{out} nevertheless

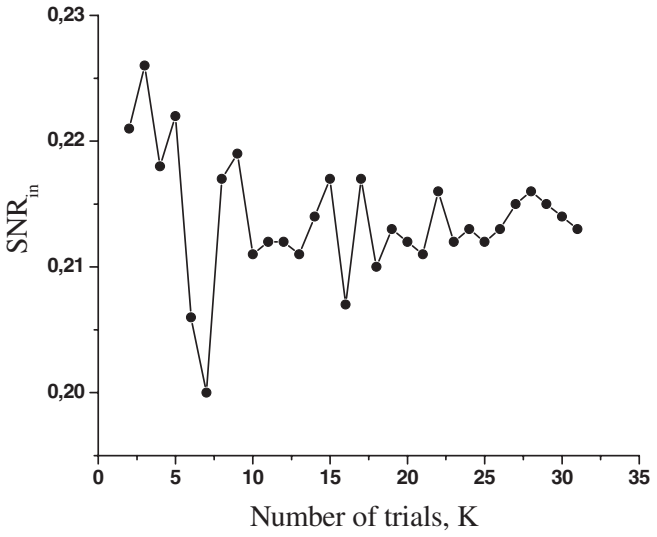

FIG. 5. Computed values of the SNR_{in} versus the number of trials K for sinusoidal GW with frequency 150 Hz and strain $h = 2^{*}10^{-23}$. The parameters of interferometer are close to those of LIGO-1, $D = 10$ cm, $d = 1$ cm, $n_2 = 10^{-13}$ $(m/V)^2$, and $r = 0.99$, detection bandwidth $f_2 = 450$ Hz, $f_1 = 50$ Hz, and the cutoff frequency is $f_c = 50$ Hz.

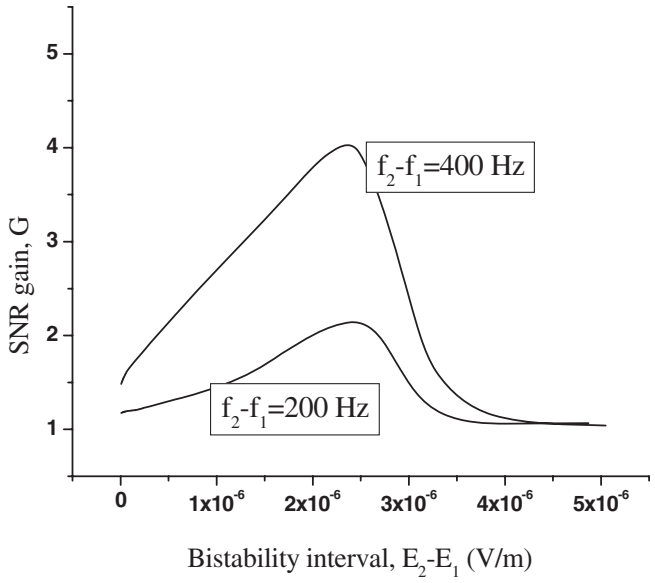

FIG. 6. SNR gain versus the bistability interval at different detection bandwidths, when detecting the sinusoidal GW with frequency $f = 150$ Hz and strain $h = 2^{*}10^{-23}$. The parameters of the interferometer are close to those of LIGO-1, $D = 10$ cm, $d = 1$ cm, $n_2 = 10^{-13}$ $(m/V)^2$, $r = 0.99$, $E_0 = 63.9054261$ V/m, $E_2 - E_1 = 2.5^{*}10^{-6}$ V/m, and the cutoff frequency is $f_c = 50$ Hz.

increases leading to the increase of SNR_{out} and G. Further decrease of the bistability interval leads to the situation when $E_2 - E_1 \ll \Delta E_{in}(t)$. Now the influence of hops in changing the ratio E_{out}/E_{in} weakens, resulting in reduction of the SNR gain. Notice that at $E_2 - E_1 = 0$ (when the NC becomes monostable), the small SNR gain is still observed: i.e. the SR mechanism performs in monostable nonlinear cavity as well, but with less efficiency.

Although the noise signal $\xi_{in}(t)$ in our study has a definite amplitude, determined by the above used noise spectrum of LIGO-1, it still would be useful to investigate the behavior of SNR_{out} when the noise amplitude is changed. To do this let us replace $\xi_{in}(t)$ in (12) and (13) by the function $B\xi_{in}(t)$, where B is a dimensionless constant coefficient. As it is known and as it follows from (14) the dependence of the SNR_{in} on the noise amplitude B goes as $\sim 1/B^2$, i.e. SNR_{in} monotonically decreases when noise amplitude increases. However, the SNR_{out} essentially differs from SNR_{in} due to the SR mechanism. To derive the behavior of SNR_{out}, let us specify again the bistability interval $E_2 - E_1 = 2.5^*10^{-6}$ V/m, corresponding to a maximum G at $B = 1$. Then by changing B we obtain the dependence of SNR_{out} versus the amplitude of input noise. The computations are performed with the number of trials $K = 1000$. As a result we obtained the graphs presented in Fig. 7. We can detect a resonancelike behavior of SNR_{out} versus input noise amplitude, which is the signature of the SR mechanism, performing here. $SNR_{out} \sim SNR_{in}$ when noise amplitude is small. However, as B is increased when $\Delta E_{in}(t)$ begins to cross the thresholds and E_{out} begins to hop from one branch to another, the SNR_{out} sharply increases, surpassing SNR_{in} at the maximum point by ~ 5 times. One also can see that the SNR gain is reduced when the detection bandwidth decreases.

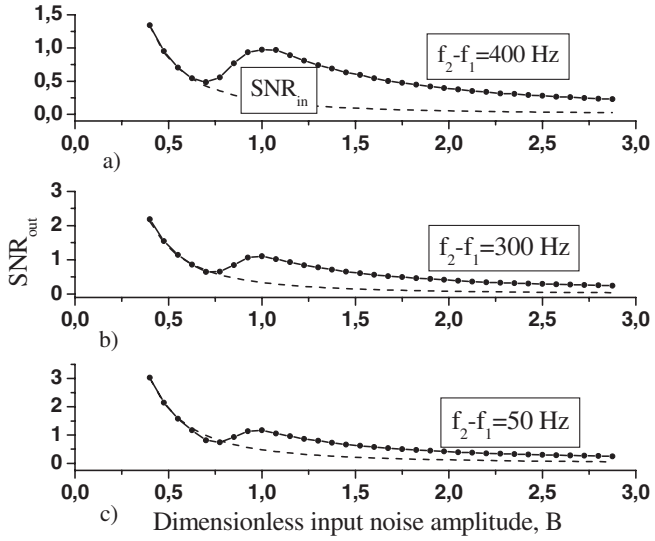

FIG. 7. Output SNR versus the amplitude of input noise (circles + line) at different detection bandwidths when a sinusoidal GW with frequency $f = 150$ Hz and strain $h = 2^*10^{-23}$ is detected. The parameters of the interferometer are close to those of LIGO-1, $D = 10$ cm, $d = 1$ cm, $n_2 = 10^{-13}$ $(m/V)^2$, $r = 0.99$, $E_0 = 63.9054261$ V/m, $E_2 - E_1 = 2.5^*10^{-6}$ V/m, and $f_c = 50$ Hz. The value $B = 1$ corresponds to the noise amplitude shown in Fig. 4(a), which is close to the LIGO-1 noise. The dashed line represents SNR_{in}.

IV. CHIRP GW

In this section we study the SNR gain for the case of GWs with chirped waveform. Such GWs are generated by compact binary systems in the final stage of inspiral, when the stars merge into a coalesced state. GW strain can be presented as the following [14]:

$$h(t) = \frac{A}{\sqrt[4]{t_{coal} - t}} \cos\left\{\left[\frac{c^3}{5\gamma M}(t_{coal} - t)\right]^{5/8}\right\}, \qquad (25)$$

where t_{coal} is coalescence time, $\gamma = 6.67^*10^{-11} n^* m^2/kg^2$ is the gravitational constant, $M = (M_1 M_2)^{3/5}/(M_1 + M_2)^{1/5}$, and M_1 and M_2 are the masses of the two stars.

Suppose that both of the stars have solar mass, $M_1 = M_2 = M_{sun} = 1.99^*10^{30}$ kg, and the amplitude $A = 7^*10^{-24}$. Figure 8 presents the waveform of $h(t)$ at the last ~ 1 sec before coalescence and its spectrum. The detection of this GW signal by LIGO-1 with the detection bandwidth $f_2 - f_1 = 450$ Hz $- 50$ Hz $= 400$ Hz is not effective, because according to (12)–(14) $SNR_{in} = 0.05$. However, by passing this noisy signal through the NC with the same parameters as in the previous section, the output SNR can be increased due to the SR mechanism. Again let us investigate first the dependence of the SNR gain on the bistability interval. As it is seen in Fig. 9 the SNR gain is

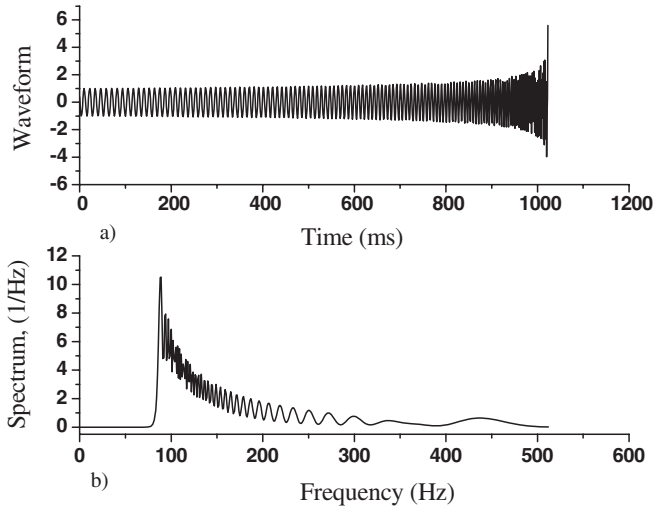

FIG. 8. Waveform and the spectrum of a chirp GW emitted by a coalesced binary system with the masses $M_1 = M_2 = M_{sun}$, at last ~ 1 sec before coalescence.

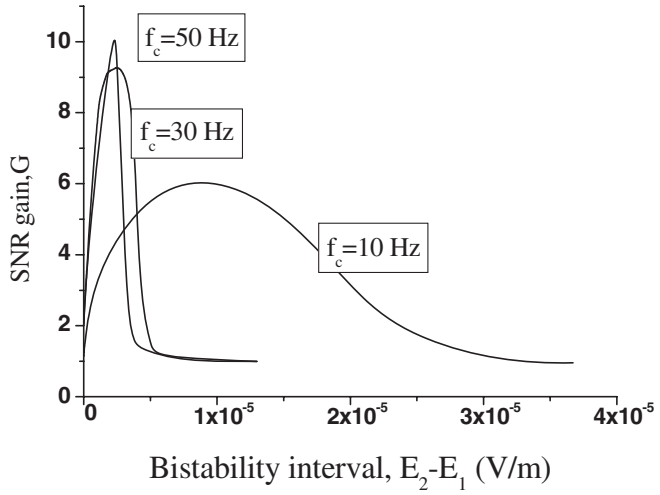

FIG. 9. SNR gain versus bistability interval at different cutoff frequencies, when detecting the chirp GW with $A = 7^{*}10^{-24}$. The parameters of the interferometer are close to those of LIGO-1, $D = 10$ cm, $d = 1$ cm, $n_2 = 10^{-13}$ (m/V)^2, $r = 0.99$, $E_0 = 63.9054261$ V/m, $E_2 - E_1 = 2.5^{*}10^{-6}$ V/m, and the detection bandwidth is $f_2 = 450$ Hz, $f_1 = 50$ Hz.

$G \sim 10$ for the cutoff frequency $f_c = 50$ Hz and the detection bandwidth $f_2 - f_1 = 400$ Hz. By decreasing the detection bandwidth, the SNR gain decreases tending to 1, which is analogous to the previous case of sinusoidal GW, so these graphs are not shown here. Instead we present the graphs corresponding to different cutoff frequencies to see how the SNR gain deteriorates when the cutoff frequency of the compensation scheme decreases. It is seen that the bistability interval where the SNR gain is observed increases, and the maximal SNR gain decreases when the cutoff frequency decreases. However, even at $f_c = 10$ Hz, the SR mechanism successfully performs here, providing a SNR gain of $\sim$6.5. Calculations of $\mathrm{SNR_{out}}$ were made analogously to those of the previous section, with the number of trials $K = 1000$. Finally, we investigated $\mathrm{SNR_{out}}$ versus the amplitude of input noise, by replacing analogously to the previous case, input noise amplitude $\xi_{\mathrm{in}}(t)$ by the $B\xi_{\mathrm{in}}(t)$. As a result, analogous graphs representing the dependence of $\mathrm{SNR_{out}}$ versus B are derived (see Fig. 10). Resonancelike behavior of $\mathrm{SNR_{out}}$ is observed, which provides the increase of $\mathrm{SNR_{out}}$ to a value $\sim$0.5 (SNR gain is $G \sim 10$). Thus the SR mechanism performs more effectively when detecting chirp GW signal rather than GW signal with the sinusoidal waveform.

In conclusion, we investigated the application of the SR phenomenon in a GW interferometer in order to increase the sensitivity. It is done by passing the output signal through a nonlinear cavity installed in the output of the interferometer. When appropriately tuned, the NC becomes capable of increasing the SNR of a noisy signal passing through it due to the SR phenomenon. We performed detailed computations of SNR gain for two types of GW waveform—sinusoidal and chirp—taking as an example the parameters of the interferometer close to those of LIGO-1. It is obtained that the influence of SR is the most effective for wideband (several hundred Hz) detection of a chirp GW signal, when a bistable regime in the NC is established. Then, passing through the NC increases the $\mathrm{SNR_{in}}$ of the interferometer output signal from $\mathrm{SNR_{in}} \sim 0.05$ to $\mathrm{SNR_{out}} \sim 0.5$. This enhancement of the SNR is not dependent on noise type, which dominates in the interferometer. The proposed approach can be used for upgrading GW interferometers.

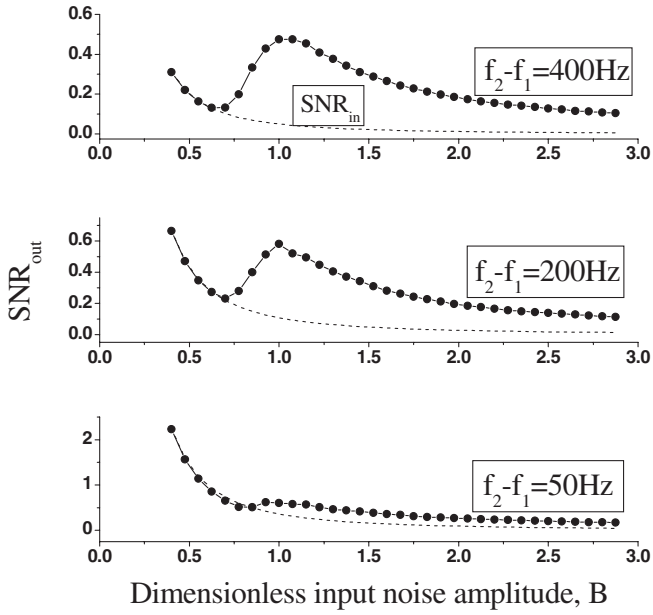

FIG. 10. Output SNR versus the amplitude of input noise (circles + line) at different detection bandwidths when a chirp GW is detected. The parameters of the interferometer are close to those of LIGO-1, $D = 10$ cm, $d = 1$ cm, $n_2 = 10^{-13}$ (m/V)^2, $r = 0.99$, $E_0 = 63.9054261$ V/m, $E_2 - E_1 = 2.5^{*}10^{-6}$ V/m, and $f_c = 50$ Hz. The value $B = 1$ corresponds to the noise amplitude shown in Fig. 4(a). The dashed line represents $\mathrm{SNR_{in}}$.

ACKNOWLEDGMENTS

I thank Professor A. Chilingarian for fruitful discussions and Ph.D. student A. Hakobyan for help in the preparation of figures. This work was supported by the Armenian National Science and Education Fund (ANSEF).

[1] B. Abbot *et al.*, Phys. Rev. D **69**, 122001 (2004).
[2] K. Belezynski, V. Kalogera, and T. Bulik, Astrophys. J. **572**, 407 (2002).
[3] The advanced LIGO web site www.ligo.caltech.edu/advLIGO/.
[4] H. J. Kimble *et al.*, Phys. Rev. D **65**, 022002 (2002); K. McKenzie, D. Shaddock, and D. McClelland, Phys. Rev. Lett. **88**, 231102 (2002).
[5] V. B. Braginski *et al.*, Phys. Rev. D **61**, 044002 (2000).
[6] A. Buonanno and Y. Chen, Phys. Rev. D **64**, 042006 (2001).
[7] K.-X. Sun, M. M. Feiger, E. Gustafson, and R. L. Byer, Phys. Rev. Lett. **76**, 3053 (1996).
[8] A. Wicht *et al.*, Opt. Commun. **134**, 431 (1997); **179**, 107 (2000); G. G. Karapetyan, Opt. Commun. **219**, 335 (2003).
[9] G. G. Karapetyan, Opt. Commun. **238**, 35 (2004).
[10] R. Benzi, A. Sutera, and A. Vulpani, J. Phys. A **14** L453 (1981); L. Gammaitoni *et al.*, Rev. Mod. Phys. **70**, 223 (1998).
[11] A. Yariv and P. Yeh, *Optical Waves in Crystals: Propagation and Control of Laser Radiation* (Wiley-Interscience, New York, 1983).
[12] H. M. Gibbs, *Optical Bistability. Controlling Lioght with Light* (Academic Press, New York, 1985).
[13] H. Wang, D. Goorskey, and M. Xiao, Phys. Rev. Lett. **87**, 073601 (2001); Phys. Rev. A **65**, 041801 (2002).
[14] S. Droz *et al.*, Phys. Rev. D **59**, 124016 (1999).